SME Annual Conference
Feb. 26 - Mar. 01, 2023, Denver, CO

Preprint 23-023

ANALYSIS OF STEEL PROPS UNDER DIFFERENT LOADING SCENARIOS

K. Mohamed, CDC NIOSH, Pittsburgh, PA
T. Batchler, CDC NIOSH, Pittsburgh, PA
T. Matthews, CDC NIOSH, Pittsburgh, PA
D. McElhinney, CDC NIOSH, Pittsburgh, PA

ABSTRACT

Steel props are a type of standing support utilized in coal mines to support mine roof. In addition to the vertical roof loading, sometimes the steel props are subjected to lateral loading of spalled ribs. To enhance the safety of mine workers, the performance characteristics of the steel prop was studied under different scenarios of vertical and lateral loadings.

Quik Stik props were used for use in this study. A uniaxial compression loading test was conducted for the Quik Stik prop assembly (inner and outer tubes, ball bearings, collar) to investigate the loading mechanism of the prop. Rupture tests were conducted for the inner and outer steel tubes of the Quik Stik props to estimate the yielding strength of the steel tubes. Nine Quik Stik props of 8-ft high were tested using the Mine Roof Simulator (MRS) at the National Institute for Occupational Safety and Health (NIOSH) Pittsburgh research facility. Three props were tested under vertical loading to measure the vertical loading capacity of the props. Six props were tested under lateral loadings with low and high roof-to-floor convergences to measure the lateral loading capacity and the retained vertical loading capacity of the props during lateral loading.

Vertical loading tests showed that the tested props could be classified as yieldable supports with a stable load capacity of about 110 kips to 140 kips. Lateral loading tests showed that the vertical load capacities of the tested props were diminished because of applying lateral loads, and the props behaved as nonyielding supports with a maximum lateral load capacity of about 8.5 kips to 9.5 kips at stable lateral displacement up to 3 inches.

INTRODUCTION

Standing supports, such as steel props and timber posts, are utilized mainly in underground coal mines as roof supports. Figure 1 shows steel set and posts were used as secondary supports in a long-term track entry in a room and pillar coal mine. Whenever roof bolters are unavailable for roof and rib bolting, standing support systems can sometimes be used to stabilize fractured rib brows (Figure 2a) or to restrain detached rib slabs to hold spalling material in place (Figure 2b). In such cases, when the spalled rib leans on the standing supports (Figure 3), the standing supports provide a lateral resisting force, increasing rib confinement and impeding further rib failure. When standing supports are used for rib control, it is essential that they be secured in such a manner that a hazard is not created as a result of dislodged support. Unexpected consequences could result from ignoring the lateral load applied on standing supports, which is a factor that could determine the stability of standing supports. For example, in a room-and-pillar coal mine, when standing supports were dislodged by a fallen rib, one of the supports struck a miner resulting in fatal injuries [1].

The Mine Roof Simulator (MRS) is a unique load frame that helps for the development and performance evaluation of support systems. The MRS closely simulates the in-service load conditions in the underground coal mines. Since the 1980s, the MRS has been used to test the response (strength, stiffness, and stability) of various support systems for a wide range of load scenarios: uniform vertical loading, asymmetric vertical loading, and biaxial loading [2]. To the best of the authors' knowledge, minimal research has been done to assess the performance characteristics of standing support systems for resisting lateral load. Previous research investigated the effect of lateral displacements (simulating floor heave) on wood crib stability by controlled biaxial displacement of full-scale wood crib supports [3].

Figure 1. Steel set and posts in track entry

(a) Supported rib brow (b) Supported rib slab

Figure 2. Standing supports used to support rib brow and to confine rib slab.

Spearing [4] evaluated the various concepts that have been developed in coal mines to provide easy height adjustment standing supports that undergo stable yielding. The designs of Quik Stik and Ball Buster supports were discussed. The Quik Stik and Ball Buster supports were tested in the MRS to determine their vertical capacities and stiffnesses. The Quik Stik props were classified as nonyielding supports, while the Ball Buster props were classified as yieldable supports. The test results of Quik Stik props were not published in this study. Chen et al. [6] introduced a mechanical yielding steel prop (MYSP) of similar design to the Ball Buster. The prop was designed to sustain large deformation in the field. The MYSP used double-layer steel ball bearings, while the Ball Buster props use single-layer of ball bearings. A greater load capacity was achieved for double-layer design. The study showed that the load capacity of the MYSP props could be controlled by changing the yielding strength of the inner and outer tubes of the prop.

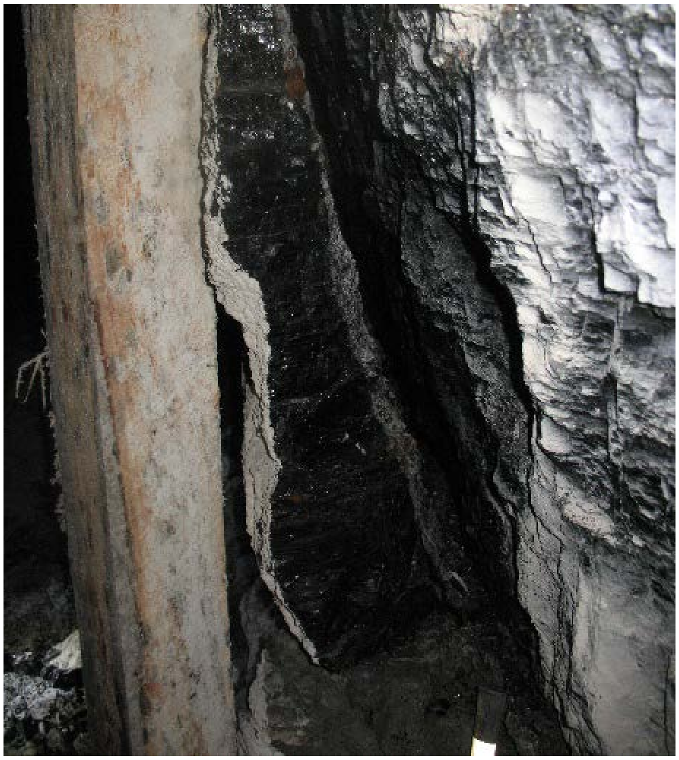

Figure 3. Standing constrains dislodged rib.

Mohamed et al. [5] initiated a testing program for different types of standing supports to provide information regarding the lateral loading capacities of standing supports. Many standing support providers were contacted and some of them were willing to supply samples of standing supports. This study is not intended to endorse a particular type of standing supports nor to provide a comparison between different types of standing supports. The key factors affecting the response of standing supports subjected to lateral loading will be studied in this testing program. These factors include the type of standing support (steel and timber), support geometry (shape, dimension), support structure (single-component or multiple-components), spatial location of the lateral load along the support, and end-conditions of support (rock strength). The performance characteristics of one type of steel props under vertical and lateral loading conditions were studied [5]. The MRS was used to determine the response of steel props to vertical and lateral loadings. Finite element models (FEMs) were then developed using the tested steel props. Steel prop models were used to study the effect of a wide range of roof and floor materials (gray shale, shale, and claystone) on the critical buckling loads of the steel props. The critical buckling load for steel props setting up against a claystone roof and floor was found to be one-half of that shown by the MRS test where roof and floor platens are made of steel. Minimum prop performance was observed when the lateral load was applied at the mid-height of the steel prop, especially at small lateral displacement (less than 2 in). In this paper, another type of standing support, Quik Stik prop, was studied.

PROBLEM DESCRIPTION AND RESEARCH METHODOLOGY

In this paper, the lateral load effects on the rated vertical capacity of a multiple-component steel prop (Quik Stik) prop are studied. The following key research questions concerning the Quik Stik prop (Figure 4), are addressed:

I. What is the lateral loading capacity of the Quik Stik prop?
II. Does lateral loading affect the rated vertical loading capacity of the Quik Stik prop?
III. Does lateral loading affect the yielding mechanism of the Quik Stik prop?

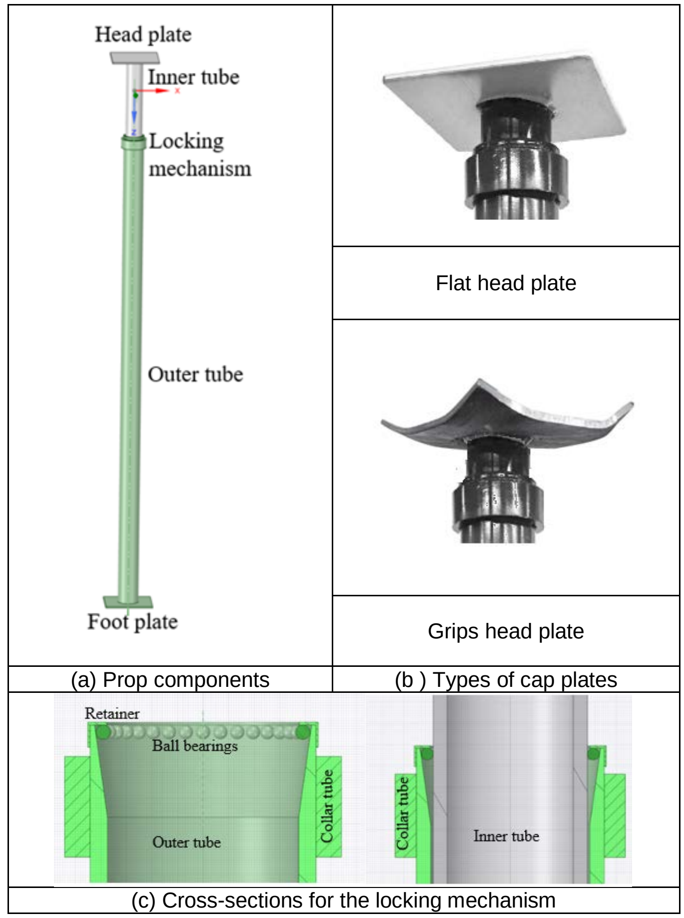

Figure 4. Components of Quik Stik prop.

The manufacturer of the Quik Stik prop states that the prop is used in underground coal mines for supporting mine roof in different locations such as headgate and tailgate entries, intersections, and bleeder entries [7]. The Quik Stik props have been used to support mine roof in recovery rooms of longwall mines. Heinzman props, version of Quik Stik prop, were used as secondary supports in a long-term track entry in a room and pillar coal mine (please see the standing supports adjacent to the right rib of the entry shown in Figure 1). The Quik Stik prop used in this study consists of two telescopic sections of tubes with a beveled section on the upper end of the outer tube that contains 36 ball bearings (Figure 4a). The lengths of inner and outer tubes are 36 in and 82 in, respectively. The outer diameters of inner and outer tubes are 2.897 in and 3.506 in, respectively. The wall thicknesses of the inner and outer tubes are 0.270 in each. An 8-inch square cap and foot boards of 0.223-inch thickness are welded to the ends of the inner and outer tubes (Figure 4b). The locking mechanism of the Quik Stik prop is composed of steel ball bearings of 0.220-inch diameter between the inner tube and the tapered surface of the outer tube (Figure 4c). The outer tube is stiffened and strengthened by a 1.540-inch-thick collar tube of 4.27-inch outer diameter and 0.393-inch wall thickness (Figure 4c). A 0.039-inch-thick retainer is welded at the top end of the outer tube to prevent the ball bearings from falling during prop handling (Figure 4c). The inner and outer tubes are made of ASTM A-513 steel Type 1. The collar tube is made of DOM1026 steel.

To answer the preceding questions, the following four steps were followed:

i. Three-point flexure tests were conducted for specimens cut from the inner and outer tubes of the Quik Stik prop to calculate the yield strength of the ASTM A-513 steel Type 1. ANSYS [8] FE models were created for the conducted flexure tests to back-calculate the complete stress-strain behavior of the ASTM A-513 steel Type 1.

ii. A uniaxial compression test was conducted for the Quik Stik prop assembly (inner and outer tubes, ball bearings, collar) to investigate the loading mechanism of the Quik Stik prop under vertical loading.

iii. Vertical loading tests were conducted for 8-ft height Quik Stik props using the MRS to determine the vertical loading capacity of the tested props.

iv. The capability of the MRS test facility has been extended to include lateral testing for standing supports. Two types of lateral loading tests were conducted for the Quik Stik props under two values of roof-to-floor convergences. At low roof-to-floor convergence, the prop is subjected to a small vertical load of about 20-25% of the prop capacity, while at high roof-to-floor convergence condition, the prop is subjected to a higher vertical load of about 45-50 % of the prop capacity. Lateral loading tests were performed in two methods. In the first method, the applied lateral load is monotonically increasing until the prop became unstable. In the second method, the applied lateral load is manually controlled to stay within a predefined narrow range while the prop is loaded vertically.

DETERMINATION OF THE MATERIAL PROPERTIES OF INNER AND OUTER TUBES OF THE QUIK STIK PROPS

The props-controlled yield design allows the ball bearings to gouge into the inner and outer tubes as the props resist roof sagging while the ball bearings and collar stays elastic. Therefore, the knowledge of the mechanical properties of the mechanical properties of inner and outer tubes are essential for any subsequent analysis for the tested Quik Stik props. Flexure tests for 32-inch-long specimens were conducted for three outer tubes and one inner tube. Figure 5 shows the setup for a 3-point flexure test conducted for the inner tube.

(1) Reaction frames (2) Roller supports (3) Loading roller (4) Inner tube specimen (5) Displacement gauges

Figure 5. Setup for 3-point flexure test for inner tube.

ANSYS FEMs were created for the conducted flexure tests to back-calculate the stress-strain relationship for inner and outer tubes. The complete stress-strain relationship of the ASTM A-513 steel Type 1 was calculated using the generalized Ramberg-Osgood equation (Equation 1) and assuming that the yield strength be at 0.2% offset strain [4]. A trial-and-error process was used to define the yield strength of the ASTM A-513 steel Type 1 which yields a good match between the finite element (FE) models and flexure tests. A good comparison between the FE and conducted flexure tests (Figure 6) was achieved by assuming the nonlinear stress-strain relationship illustrated in Figure 7.

$$\varepsilon = \frac{\sigma}{E} + 0.002 \times \left(\frac{\sigma}{\sigma_{YS}}\right)^{1/n} \qquad \text{Equation (1)}$$

where

σ is the stress in psi,

ε is the strain, in/in,

E is young's modulus, which it is assumed to be 29x106 psi,

σYS is the yield strength, which it is assumed to be 75 ksi, and

"n" is a constant describing the hardening behavior of the material. The best match between FE models and buckling tests for steel props was achieved by assuming "n" constant equals to 0.143.

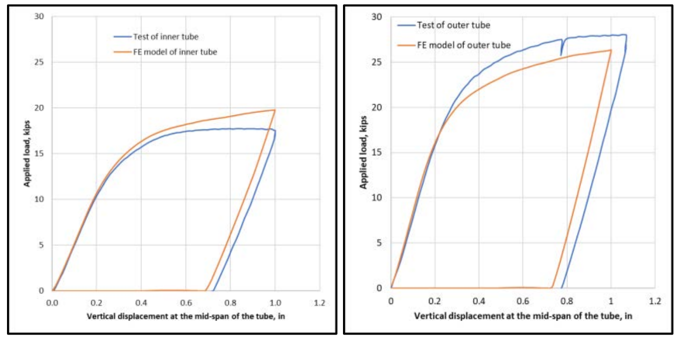

Inner tubes outer tubes

Figure 6. Load-displacement curves for 3-point flexure tests of inner and outer tubes.

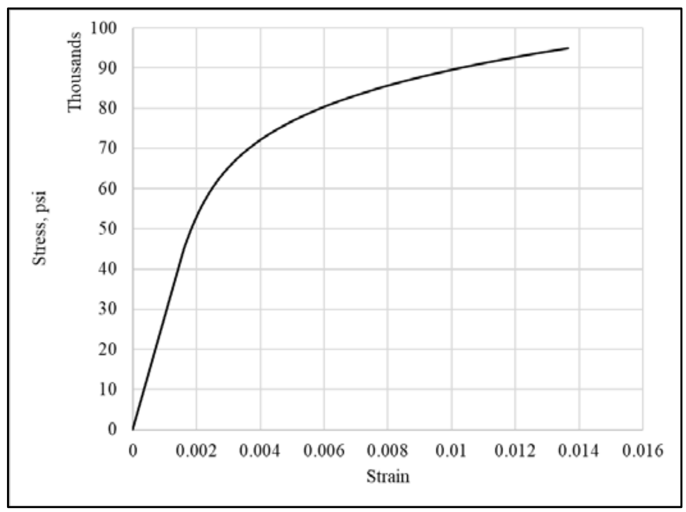

Figure 7. Stress-strain curve of ASTM A-513 steel tubes.

LOADING MECHANISM OF QUIK STIK PROP

A uniaxial compression test was conducted for the Quik Stik prop assembly (inner and outer tubes, ball bearings, and collar) to explain the loading mechanism of the Quik Stik prop under vertical loading (see Figure 8a). Before starting the test, the ball bearings were uniformly distributed between the outer and inner tubes (Figure 8b). Once vertical pressure is applied, the ball bearings engage the steel tubes and lock the unit in place, allowing it to accept loading immediately. The test specimen was placed in the MRS with full roof and floor contact to establish uniform loading on the support (Figure 8a). To simulate the convergence of the mine roof and floor, a controlled vertical displacement was applied at a slow rate of 0.05 inches/minute to the test specimen by the MRS load frame. The convergence of the roof and floor platens of the MRS continued up to 2.5 inches of vertical displacement (Figure 8c). The yielding mechanism is achieved mainly by the gouging of the ball bearings on the inner and outer tubes as convergence occurred (Figure 8d and 8e).

The load-displacement curve for the Quik Stik prop assembly is shown in the orange color curve in Figure 9. As mentioned earlier, the compression test of the Quik Stik assembly was conducted for a vertical displacement of 2.5 inches which was not enough to explain the complete loading mechanism of the prop. There were not sufficient props to redo the compression test for a larger vertical displacement. To explain the complete loading mechanism of the prop, the load-displacement curve was obtained from the vertical compression test of a full-scale prop of 8-ft high. The load-displacement curve of a full-scale Prop 1 (black color curve in Figure 9) was superimposed into that of the Quik Stik prop assembly. The full-scale prop test will be discussed in detail in the next section. The load-displacement curves of the Quik Stik prop assembly and the full-scale prop coincide as shown in Figure 9.

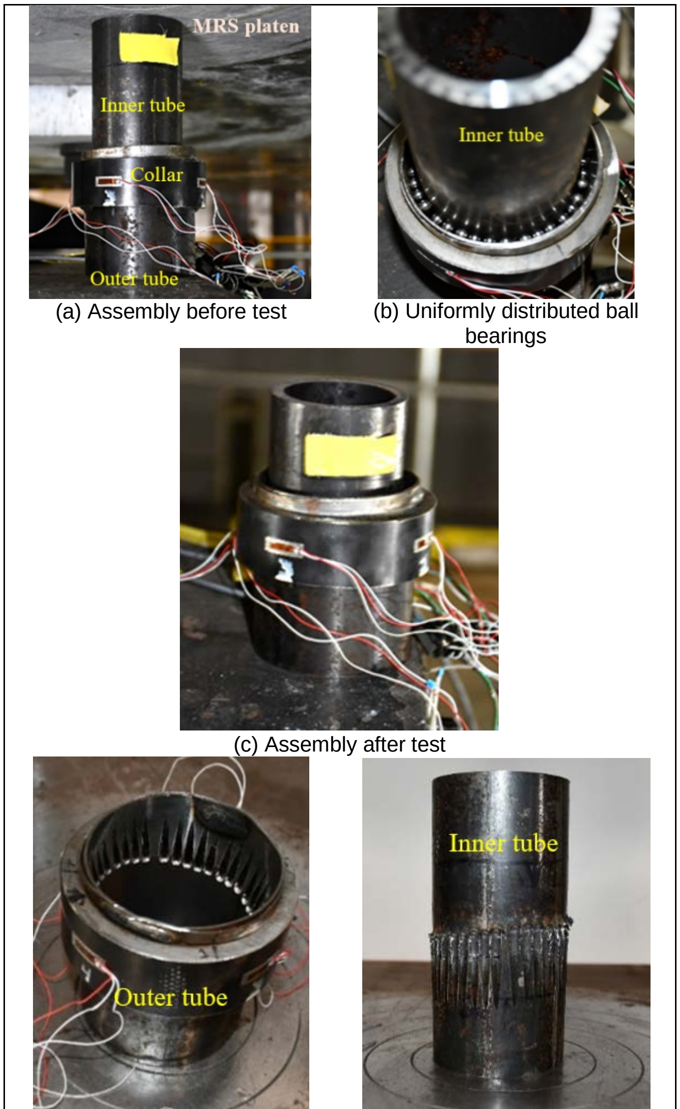

(a) Assembly before test (b) Uniformly distributed ball bearings
(c) Assembly after test
(d) Indentation marks in outer tube (e) Indentation marks in inner tube

Figure 8. Uniaxial compression test of Quik Stik prop assembly.

When the Quik Stik prop is subjected to vertical load, four stages of loadings were identified in the load-displacement curve (a-b, b-c, c-d, and d-e in Figure 10). Schematic drawings for those four stages are illustrated in Figure 10 explaining the loading mechanism of the Quik Stik prop. The initial stage is represented on the load-displacement curve from the initial point "a" until point "b" which is approximately 1-inch of displacement. During this stage, the support slightly yields as the ball bearings start to gouge into the inner tube and the beveled section of the outer tube. At point "b" the maximum embedded depth in both inner and outer tubes is achieved. As the vertical displacement is further increased to about 2 inches, the outer tube, which is reinforced by the collar, increases its resistance to further deformation. Detailed investigation for the role of the collar in loading mechanism of Quik Prop will be presented in the next section. At point "c" the ball bearings arrived at the beveled edge of the outer tube, and they temporarily stuck into the outer tube (Figure 10c). During the next stage of loading from point "c" to "d", the ball bearings and the outer tube moved together as a unit while the ball bearing continued gouging in the inner tube. At point "d" the inner tube deforms to such an extent that the ball bearings can pass by the beveled edge of the outer tube (Figure 10d). At this final state of yielding from point "d" to "e" and until the end of the test, the ball bearings are gouging into both the inner and outer tubes through alternated stick and slip type mechanisms. As one tube strain hardens from the increase stress, it allows the ball bearing to gouge the other tube. This process then alternates between the inner and outer tubes and acts as a stick-slip yield mechanism (Figure 10e).

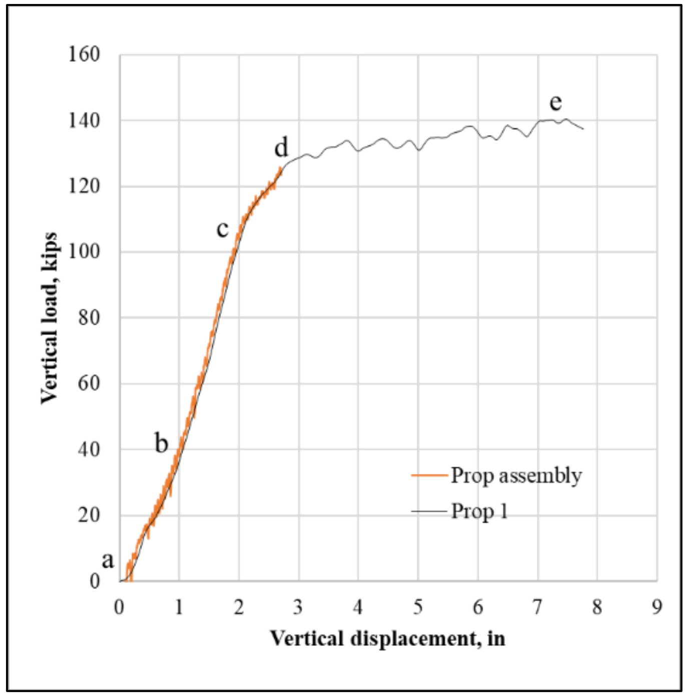

Figure 9. Load-displacement curve of the Quik Stik prop assembly.

FULL-SCALE TESTING FOR QUIK STIK PROPS

Full-scale testing of steel props represents the real condition in coal mines. This study conducted full-scale vertical and lateral loading testing for Quik Stik steel props using the MRS.

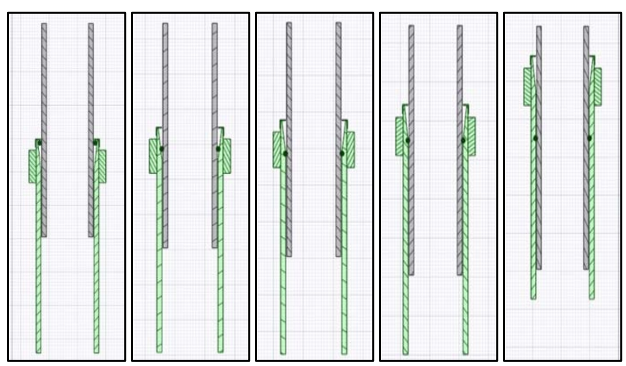
(a) (b) (c) (d) (e)

Figure 10. Vertical loading stages of Quik Stik prop.

Vertical load capacity tests

The objective of this test is to establish a baseline performance for the tested Quik Stik props under vertical loading and to investigate the effect of collar on the performance of the Quik Stik prop. Three Quik Stik props of 8-ft height were tested; Props 1 and 3 were with a flat head plate (Figure 11a and 11c) and Prop 2 was with a grips head plate (Figure 11b). The collar of Prop 3 was carefully separated from the outer pipe of the prop without damaging the outer tube (Figure 11c). Removing the collar of Quik Stik Prop 3 makes it likes Ball Buster prop.

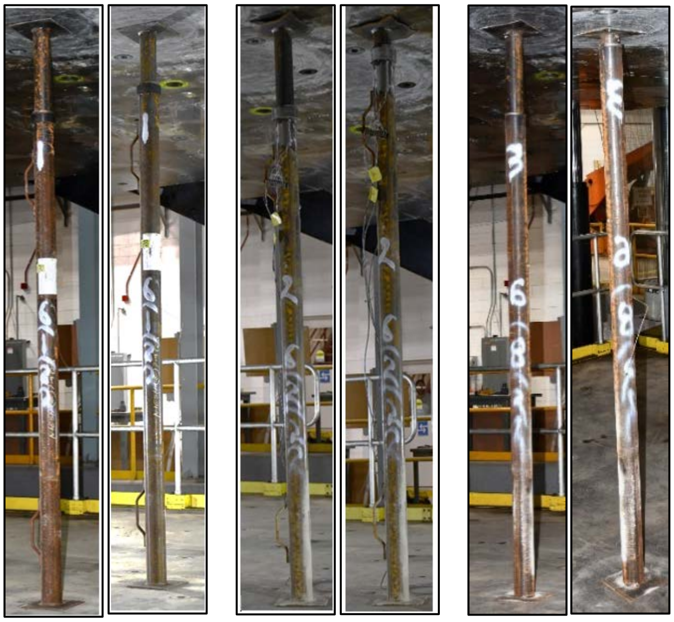

Before After test Before After test Before After test
(a) Prop 1 (b) Prop 2 (c) Prop 3

Figure 11. Vertical loading tests for Props 1, 2 and 3.

To simulate the convergence of the mine roof and floor, a controlled vertical displacement was applied at a rate of 0.05 inches/minute to the prop by the load frame of the MRS. The load-displacement curves for Props 1, 2 and 3 are shown in Figure 12. Unlike props 1 and 3, the load-displacement curve of Prop 2 initially concaved upward because of the deformation of the curved head plate. This grips head plate is intended to dig into the roof to help to secure it in place. The flat head plate probably wouldn't happen (at least as quickly) in "softer" mine roof compared to the rigid MRS platen. During this early stage of loading the curved head plate of Prop 2 became flat, then the prop gained the same stiffness as Prop 1, but it did not reach the same vertical load capacity as Prop 1. Prop 1 and Prop 2 show perfect yielding behavior with ultimate capacities of 110 kips and 140 kips, respectively. The tests were terminated at a maximum vertical displacement of 8 inches, even if they could be continued with more displacement with constant vertical load capacity. Therefore, the tested Quik Stik props are classified in this study as yieldable supports. Figure 12 shows that Props 1 and 3 have similar stiffnesses at early stage of loading then Prop 3 showed smaller stuffiness and ultimate loading capacity. The collar of Quik Stik prop confines the lateral deformation of outer pipe, therefore it increases the stiffness and ultimate vertical capacity of the prop.

Buckling analysis was conducted for the tested 8-ft-high inner tube assuming a clamped boundary condition. The slenderness ratio of the tested props is calculated as 51.45. For yielding strength of 75 ksi, the critical slenderness ratio is 62.83 (greater than the calculated slenderness ratio). Therefore, the tested prop is classified as a short column. The critical buckling load was calculated as 252 kips, which is about 1.8 times the tested prop capacity. This result explains why the tested props did not buckle as shown in the pictures of the props after testing (see Figure 11).

After testing, the outer tubes of Props 1 and 2 were cut into halves to investigate the indentation patterns created because of the gouging of ball bearings into the tubes. Figure 13 shows the indentation patterns in the inner and outer tubes of Props 1 and 2. Unlike the prop assembly test (Figure 8), the indentation patterns of Props 1 and 2 did not show uniform spacings. One-half of the outer tubes showed close-spacing indentation marks, while the other half showed few indentation marks which means that the loading conditions of tested props were asymmetric. Despite the asymmetric loading condition of Prop 1, the load-displacement curves of Prop 1 and the prop assembly test coincided with up to a vertical displacement of about 3.0 inches (Figure 9).

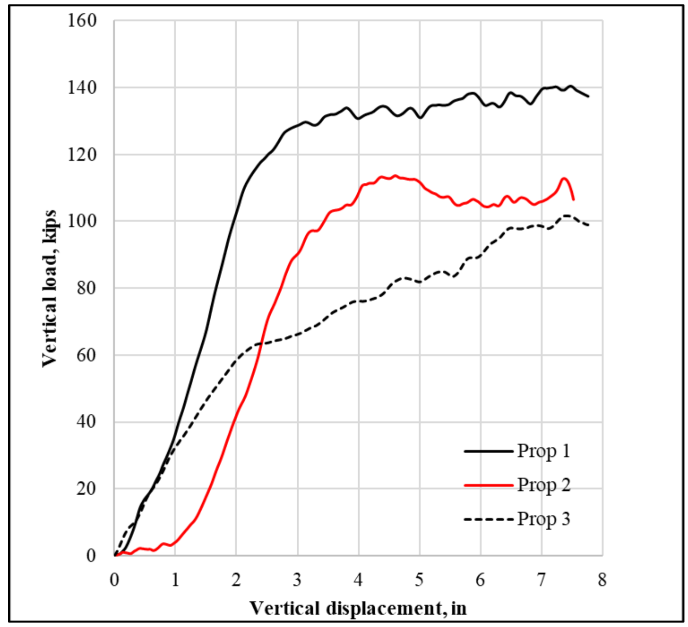

Figure 12. Vertical load-displacement curves for Props 1, 2 and 3.

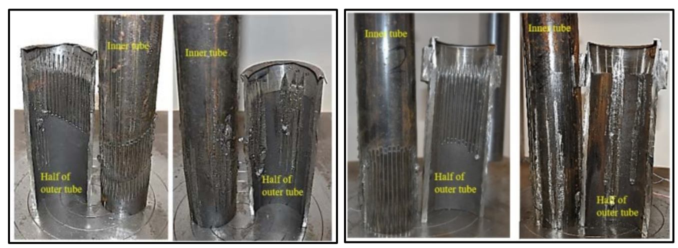

(a)Prop 1 (b) Prop 2

Figure 13. Indentation marks for Props 1 and 2.

Lateral load capacity tests

MRS was used to conduct testing of Quik Stik props for lateral load capacity. The lateral load tests mimic the static loading scenario of friable/blocky sloughed ribs in which a collapsed rib leaned against the prop, then the fallen rib disintegrates into pieces releasing the lateral load while the prop is still supporting the mine roof (see Figure 1). In this study, it is assumed that the initial rib fall against the prop does not create any sort of "impact" loading with the full weight of the roof rock that would represent a different loading scenario used in the study. Dynamic/impact loading will be investigated in near future by using numerical modeling technique. A lateral loading fixture was attached to the floor platen of the MRS (see Figure 14) and used to apply lateral loading on tested steel props. The lateral load was generated via a hydraulic cylinder mounted on the lateral loading frame. The height of the fixture is about 6-ft high, and the position of the hydraulic cylinder is adjustable so that the lateral load can be applied at the mid-height of the tested prop.

Prop 4 and Prop 7 were tested to determine the lateral load capacity of Quik Stik props at designated vertical preloads. The tested props are 8-ft-high props of flat head plates. A high vertical preload of 70 kips (about 50% of the vertical capacity of the prop) was applied on Prop 4 (Figure 14a). Then, a gradually increased lateral load was applied at the mid-height of the prop. The prop slightly bowed at a maximum lateral load of about 9 kips (Figure 14b). With further lateral load, the prop became unstable and dislodged at the head plate (Figure 14c). Then, the prop was reinstalled for loading it vertically to measure the retained vertical loading capacity and to define its loading behavior. During the reload stage, no lateral load was applied. The final prop configuration showed that the prop buckled at its mid-height with a lateral displacement of about 6 inches (Figure 15a).

(a) pre-vertical loading (b) lateral loading

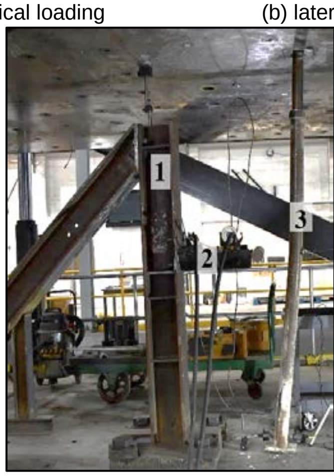

(c) slipped prop

(1) Lateral loading fixture mounted on the floor of the MRS
(2) hydraulic loading ram
(3) Tested prop

Figure 14. Configurations of Prop 4 at different stages of loadings.

(a) Prop 4 (b) Prop 5 (c) Prop 6 (d) Prop 7 e) Prop 8 f) Prop 9

Figure 15. Final configurations for tested props.

The same testing procedure of Prop 4 was applied for Prop 7, except a low vertical preload of about 30 kips (about 20% of the vertical capacity of the prop) was applied on Prop 7. The final prop configuration showed that the prop buckled at its mid-height with a lateral displacement of about 6.5 inches (Figure 15d). The tests conducted for Props 4 and 7 mimic the loading scenario of friable/blocky sloughed ribs in which a collapsed rib leaned against the prop, then the fallen rib disintegrates into pieces releasing the lateral load while the prop is still supporting the mine roof.

Figure 16a shows the lateral load-displacement curves for Props 4 and 7. The lateral load-displacement curves were initially linear up to lateral loads of about 4 and 2 kips for Props 4 and 7, respectively. Then, the lateral load-displacement curves became nonlinear until the props became unstable at a lateral displacement of about 3 in (see Figure 14c) and corresponding vertical displacements of about 1.7 in and 0.8 in for Props 4 and 7, respectively as shown in Figure 16b. Figure 16a shows that regardless of the amount of the vertical preload, the lateral capacity of Props 4 and 7 was about 9 kips (about 6% of the vertical load capacity of the tested props).

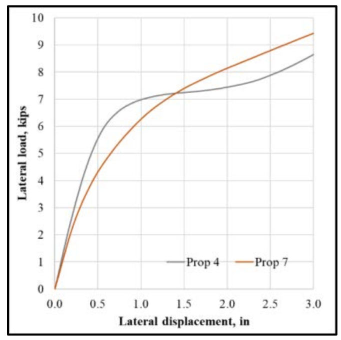

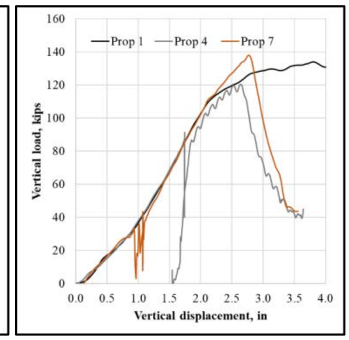

(a) Lateral (b) Vertical

Figure 16. Test results for Props 4 and 7 (load-displacement curves).

Figure 16b shows the vertical load-displacement curves for Props 4 and 7 compared with the vertical load-displacement curve of Prop 1, which was not loaded laterally. The vertical load-displacement curves for Props 1, 4, and 7 coincide for the vertical preload stages of Props 4 and 7. During the reloading stage, the vertical load-displacement curves of Props 4 and 7 followed the load-displacement curve of Prop 1. Prop 7 showed slightly lower vertical load capacity. Unlike unbuckled Prop 1, Props 4 and 7 buckled because of applying lateral load (see Figures 15a and 15d).

Figure 17 shows the indentation patterns in the inner and outer tubes of Props 4 and 7. It shows that the props were at the end of the third loading stage (see Figure 10d); this explains why the vertical load-displacement curves of Props 4 and 7 are missing the perfectly yielding portions. During the prop reloading stage, the lateral deflections of the prop prevented the ball bearings from passing into the narrow gap between the inner and outer tube. Hence, the ball bearings were stuck at the bottom of the beveled section of the outer tube. Figure 17 shows that the indentation marks of Prop 7 are more uniform compared with those of Prop 4, which indicates that unlike Prop 4, the ball bearings of Prop 7 were uniformly distributed between the inner and outer tubes but the differences between the vertical load-displacements curves of Props 4 and 7 were insignificant.

Prop 4 Prop 7

Figure 17. Indentation marks for Props 4 and 7

The tests conducted for Props 5, 6, 8, and 9 mimic the loading scenario of a toppled slabby rib leaned against the prop (see Figure 3). In such a loading scenario, the lateral load applied on the prop will be maintained while the prop is still supporting the mine roof.

Props 5, 6, 8, and 9 are 8-ft-high Quik Stik props. Only Prop 5 has a flat head plate, and the other props have grips head plates. The loading scenario adopted for loading Props 5, 6, 8, and 9 is as follows: (1) a vertical preload is applied on the prop, (2) a lateral load is applied at the mid-height of the prop, and the lateral load is manually maintained within a predefined narrow range while the prop is loaded vertically, (3) the lateral load stopped when the hydraulic jack of lateral loading reached its maximum extension (about 6 in), and (4) vertical loading continues until the prop became unstable when the test is terminated.

A high vertical preload of about 70 kips was applied on Props 5 and 6, while a low vertical preload of about 30 kips was applied on Props 8 and 9. Figure 18a shows the vertical load-displacement and curves for Prop 5 compared with Prop 1. The vertical load-displacement curves for Props 5 and 1 are in a good match for the vertical preload stage of Prop 5, which confirms the repeatability of the conducted tests. Figure 18a shows lateral load-displacement and curves for Prop 5. While Prop 5 is continued to be loaded vertically, the applied lateral load at the mid-height of the prop was maintained between 3 and 5 kips (about 45% of the lateral load capacity of the prop). During the lateral load stage, the prop started to buckle (see Figure 15b for final configuration of the prop). Therefore, the vertical load capacity reduced to a residual capacity of 15 kips.

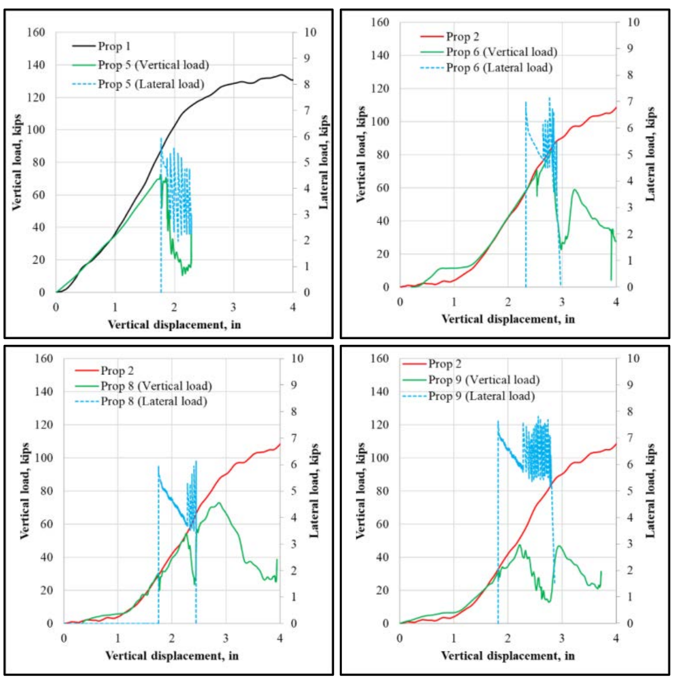

Figure 18. Test results for Props 5,6,8, and 9.

Figure 18b shows the vertical load-displacement curves for Prop 6 compared with Prop 2. The vertical load-displacement curves for Props 6 and 2 are in good agreement for the vertical preload stage of Prop 6. Figure 18b shows lateral load-displacement and curves for Prop 6. While Prop 6 is continued to be loaded vertically, the applied lateral load at the mid-height of the prop was maintained between 5 and 6 kips (about 60% of the lateral load capacity of the prop). Like Prop 5, during the lateral load stage, the Prop 6 started to buckle, and the vertical load capacity of the prop was reduced to a residual capacity of 25 kips. At this moment, the hydraulic jack of lateral loading reached its maximum extension, and the prop was still stable. With further vertical loading, the prop showed a maximum vertical load capacity of 60 kips (about 55% of the vertical load capacity of the prop) followed by softening behavior. The test was terminated when the prop became unstable (see final configuration of the prop in Figure 15c

Like Prop 6, a similar analysis was conducted for Props 8 and 9 (Figures 18c and 18d). The vertical load-displacement curves for Props 8, 9, and 2 coincide for the vertical preload stage of Props 8 and 9. The applied lateral loads for Props 8 and 9 were maintained at about 55% and 72% of the lateral load capacity of the prop, respectively. As a result of applying lateral load on Props 8 and 9, the vertical load capacity of the props dropped to about 25 and 15 kips, respectively. With further vertical loading, Props 8 and 9 showed a maximum vertical load capacity of 45 and 70 kips, respectively. The tests were terminated when the props became unstable (see final configurations of the props in Figures 15e and 15f).

Figure 19 shows the indentation patterns in the inner and outer tubes of Props 5, 6, 8, and 9. It shows that the props were at the end of the second loading stage (see Figure 10b). Therefore, the locking mechanism of the Quik Stik prop was not fully utilized for the proposed loading scenario of Props 5, 6, 8, and 9. The props were failed by the buckling mechanism rather than the designed yielding mechanism of the props.

(a) Prop 5 (b) Prop 6
(c) Prop 8 (d) Prop 9

Figure 19. Indentation marks for Props 5, 6, 8, and 9.

DISCUSSIONS AND CONCLUSION

Standing supports are mainly utilized in coal mines to support roof and are occasionally used to resist the lateral movement of spalled ribs. The National Institute for Occupational Safety and Health (NIOSH) conducted a testing program using the Quik Stik prop support to investigate the effect of lateral loading on the vertical load capacity of standing supports. The Quik Stik is a high yielding steel prop that utilizes ball bearings between two tube sections that allow height extension while preserving a high yielding capability. The yield capability is achieved by gouging of the ball bearings on the inner and outer tubes.

This study conducted a full-scale testing for an 8-ft-tall Quik Stik steel prop using NIOSH's Mine Roof Simulator (MRS). In this study, a steel fixture was attached to the floor platen of the MRS and in conjunction with a hydraulic ram used to apply lateral loading on tested props. The lateral load capacity attained by the Quik Stik was about 9 kips (about 6% of the vertical load capacity of the tested props). This study also looked at the effect of lateral load on the performance characteristics of the prop. As expected, a lateral load applied to the Quik Stik would affect the prop's vertical loading capacity. The Quik

Stik starts to bow and conceivably buckles when a lateral load is applied. When a continuous lateral load is applied, the vertical load capacity was reduced by about 55% of the "standard" rated vertical load capacity of the support. The props are designed to fail by yielding, but under lateral loading condition, they failed by buckling instead of yielding.

There are still several research areas that would benefit from further study. Do the end-conditions, such as steel platens versus strong/weak synthetic rocks, of the steel prop affect its vertical loading capacity? Does the spatial location of the lateral load along the support affect its lateral loading capacity? In addition, other types of support need to be tested. Ultimately, the type of information obtained from this study and future studies can be used to aid in developing rib design criteria and to assist mine operators in the selection and use of rib support in underground mines.

DISCLAIMER

The findings and conclusions in this study are those of the authors and do not necessarily represent the official position of the National Institute for Occupational Safety and Health (NIOSH), Centers for Disease Control and Prevention (CDC). Mention of any company or product does not constitute endorsement by NIOSH.

REFERENCES

1, MSHA (2010) Report of investigation. Fall of roof/rib. CAI-2010–38.

2. Barczak TM (1988) An overview of standing roof support practices and developments in the United States. Proceedings of the Third South African Rock Engineering Symposium, Johannesburg, Republic of South Africa: S Afr Inst Min Metall October 10–12, 2005:301–334.

3. Barczak TM and Tasillo Carol L (1988) Factors affecting strength and stability of wood cribbing: height, configuration, and horizontal displacement. Report of investigations (United States Bureau of Mines), 9168.

4. Spearing S (2008) Designing Free-Standing Steel Supports for Coal Mine Roof Support. 27th International Conference on Ground Control in Mining (ICGCM).

5. Mohamed KM and Batchler T (2022) Analysis of steel prop supports subjected to vertical and lateral loading. Mining, Metallurgy & Exploration, https://doi.org/10.1007/s42461-022-00673-2.

6. Chen Y, Pu H, Wu P, Wu H, Wu Y, Hao Y, Lai GT, Azmi A, and Abdurrahman M (2020) Mechanical properties experiment of load capacity on a mechanical yielding steel prop (MYSP) and its application in roadway support. http://dx.doi.org/10.17576/jsm-2020-4907-05.

7. Quik Stik Prop specifications, https://www.jennmar.com/files/content/products/props.pdf

8. ANSYS (2020) Documentation for ANSYS, release 20. ANSYS Inc., Canonsburg, PA